Supporting Information File

A new series of tetrahedral Co(II) complexes [$CoLX_2$] (X = NCS, Cl, Br, I) manifesting single-ion magnet features

Amit Kumar Mondal,[a] Mahesh Sundararajan*[b] and Sanjit Konar*[a]

[a] *Department of Chemistry, IISER Bhopal, Bhopal Bypass Road, Bhauri, Bhopal-462066, M. P., India.*

[b] *Theoretical Chemistry Section, Bhabha Atomic Research Centre, Mumbai 400085, India.*

Table S1. X-ray Crystallographic Data and Refinement Parameters for complexes **1**-**4**.

	1	**2**	**3**	**4**
Formula	$C_{41}H_{32}CoN_2OP_2S_2$	$C_{39}H_{32}Cl_2CoOP_2$	$C_{39}H_{32}Br_2CoOP_2$	$C_{42}H_{40}Cl_2I_2CoO_5P_2$
M_w (g mol^{-1})	753.68	708.42	797.32	1070.31
Crystal size (mm)	0.50×0.19×0.15	0.45×0.15×0.10	0.48×0.20×0.18	0.42×0.14×0.11
Crystal system	Triclinic	Monoclinic	Monoclinic	Monoclinic
Space group	*P*-1	$P2_1/c$	$P2_1/c$	$P2_1/m$
T (K)	177(2)	140(2)	140(2)	296(2)
a (Å)	9.5642(8)	16.8684(9)	16.884(2)	9.856(2)
b (Å)	10.6421(9)	10.4873(7)	10.6015(14)	18.907(4)
c (Å)	18.4548(16)	40.263(2)	40.409(5)	12.358(3)
α (°)	90.493(4)	90	90	90
β (°)	101.033(4)	111.257(3)	109.960(5)	107.427(3)
γ (°)	99.395(4)	90	90	90
V (Å^3)	1817.4(3)	6638.1(7)	6798.6(15)	2197.2(8)
Z	2	8	8	2
ρ_{calcd} (g cm^{-3})	1.377	1.418	1.558	1.618
μ(MoKα) (mm^{-1})	0.711	0.806	2.981	2.031
F(000)	778	2920	3208	1058.0
T_{max}, T_{min}	0.889, 0.860	0.933, 0.855	0.575, 0.484	0.810, 0.728
h, k, l range	$-12 \le h \le 12$, $-14 \le k \le 14$, $-24 \le l \le 24$	$-22 \le h \le 22$, $-13 \le k \le 13$, $-52 \le l \le 53$	$-22 \le h \le 22$, $-14 \le k \le 12$, $-54 \le l \le 54$	$-11 \le h \le 11$, $-22 \le k \le 22$, $-14 \le l \le 14$
Collected reflections	8946	15917	17412	4022
Independent reflections	6267	9475	9110	3311
Goodness-of-fit (GOF) on F^2	1.073	0.984	1.009	1.034
R1, wR2 ($I > 2\sigma I$)	0.0479, 0.1080	0.0561, 0.1087	0.0850, 0.1083	0.0720, 0.2056
R1, wR2 (all data)	0.0860, 0.1251	0.1254, 0.1387	0.1947, 0.1335	0.0858, 0.2208
CCDC Number	1460756	1460754	1460755	1520987

$R1 = \Sigma||Fo| - |Fc||/\Sigma|Fo|$ and $wR2 = |\Sigma w(|Fo|^2 - |Fc|^2)|/\Sigma|w(Fo)^2|^{1/2}$

Table S2. Bond distances (Å) around Co^{II} centers found in complexes **1**-**4**.

1		**2**		**3**		**4**	
Co – P2	2.369(2)	Co – P5	2.382(3)	Co – P3	2.373(1)	Co – P1	2.364(2)
Co – P1	2.375(1)	Co – P6	2.374(3)	Co – P4	2.363(2)	Co – P1′	2.364(2)
Co – N2	1.919(1)	Co – Cl1	2.237(1)	Co – Br1	2.375(1)	Co – I1	2.555(1)
Co – N1	1.930(1)	Co – Cl2	2.200(1)	Co – Br2	2.345(1)	Co – I2	2.554(1)

Table S3. Bond angles (°) around Co^{II} centers found in complexes **1**-**4**.

1		**2**		**3**		**4**	
P2–Co1–P1	112.82(4)	Cl1–Co1–Cl2	115.28(3)	Br1–Co1–Br2	117.52(2)	I2–Co1–I1	118.53(2)
P2–Co1–N2	104.80(4)	Cl1–Co1–P5	107.03(5)	Br1–Co1–P3	105.78(3)	I2–Co1–P1	105.79(2)
P2–Co1–N1	112.93(4)	Cl1–Co1–P6	103.73(5)	Br1–Co1–P4	102.91(2)	I2–Co1–P1′	105.79(3)
P1–Co1–N2	112.69(4)	Cl2–Co1–P5	108.06(5)	Br2–Co1–P3	107.27(2)	I1–Co1–P1	107.00(3)
P1–Co1–N1	99.22(3)	Cl2–Co1–P6	108.38(5)	Br2–Co1–P4	109.26(2)	I1–Co1–P1′	107.00(3)
N2–Co1–N1	114.70(3)	P5–Co1–P6	114.55(5)	P3–Co1–P4	114.32(1)	P1–Co1–P1′	112.92(2)

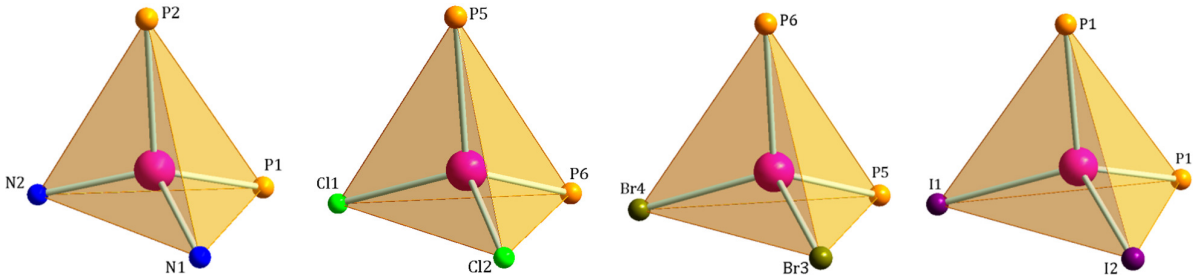

Fig. S1. Distorted tetrahedral coordination geometry around the Co^{II} centers in complexes **1-4**.

Shape analysis

Table S4: Summary of SHAPE analysis for complexes **1**-**4**.

SP-4	1	D_{4h}	Square
T-4	2	T_d	Tetrahedron
SS-4	3	C_{2v}	Seesaw
vTBPY-4	4	C_{3v}	Vacant trigonal bipyramid

Structure [ML_4]	SP-4	T-4	SS-4	vTBPY-4
Complex **1**	28.596	**0.281**	7.907	3.535
Complex **2**	28.439	**0.383**	7.771	3.393
Complex **3**	28.359	**0.519**	6.622	3.293
Complex **4**	30.728	**1.201**	7.871	3.345

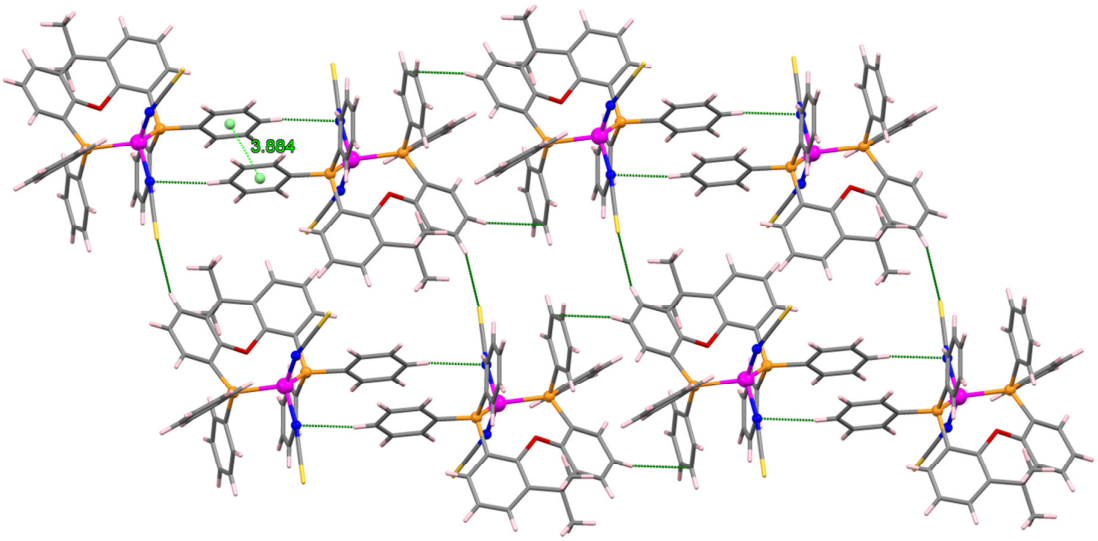

Fig. S2. A view of supramolecular 2D arrangement of complex **1** through intermolecular H-bonding and π···π interactions.

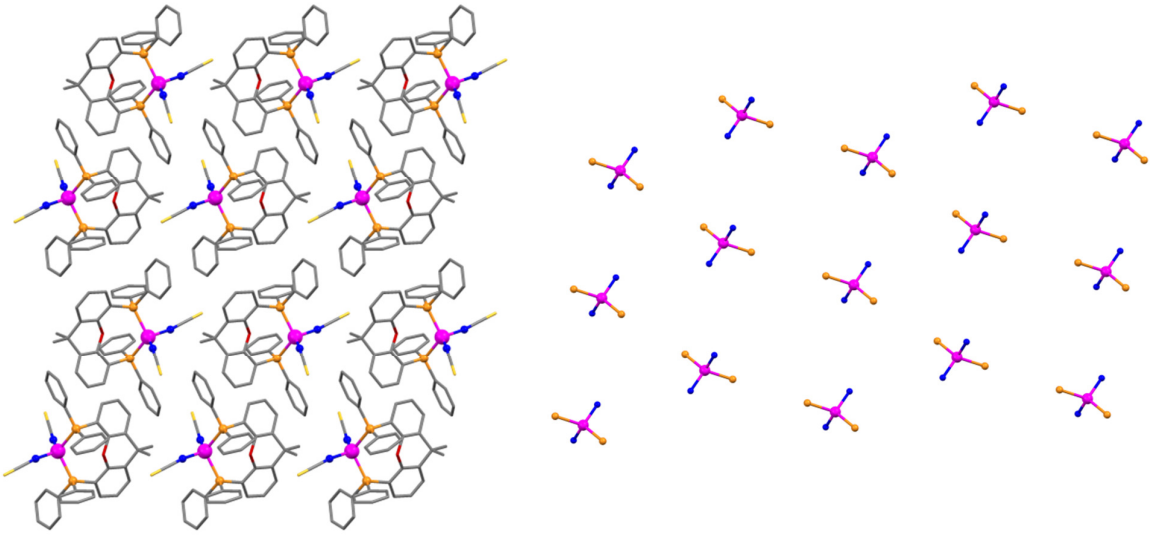

Fig. S3. Packing arrangement of complex **1** along the crystallographic *a*-axis (left); Packing arrangement of complex **1** along the crystallographic *b*-axis, after removing the outer sphere ligand and keeping only the tetrahedral Co^{II} cores (right).

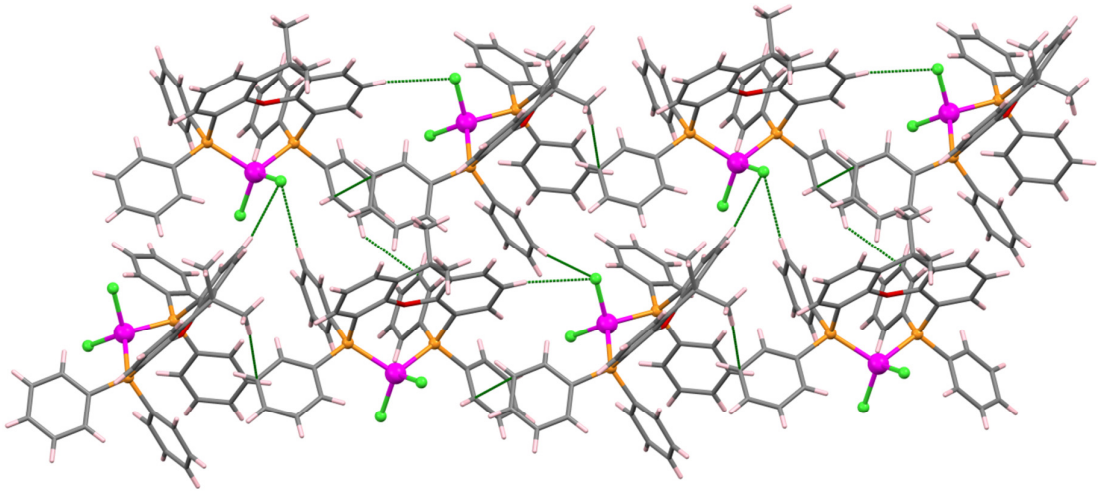

Fig. S4. A view of supramolecular 2D arrangement of complex **2** through intermolecular H-bonding and CH···π interactions.

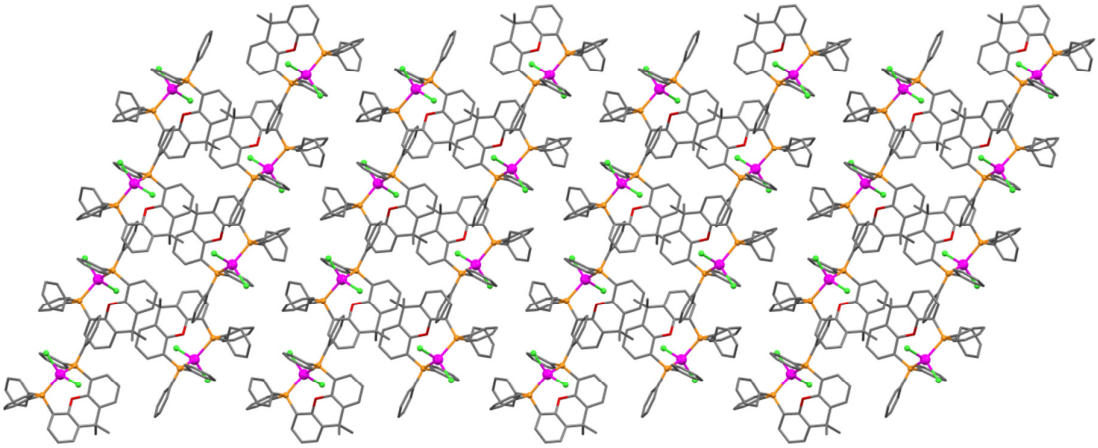

Fig. S5. Packing arrangement of complex **2** along the crystallographic *b*-axis.

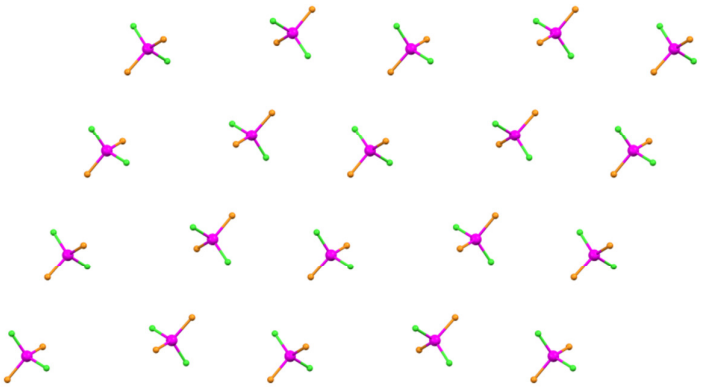

Fig. S6. Packing arrangement of complex **2** along the crystallographic *b*-axis, after removing the outer sphere ligand and keeping only the tetrahedral Co^{II} cores.

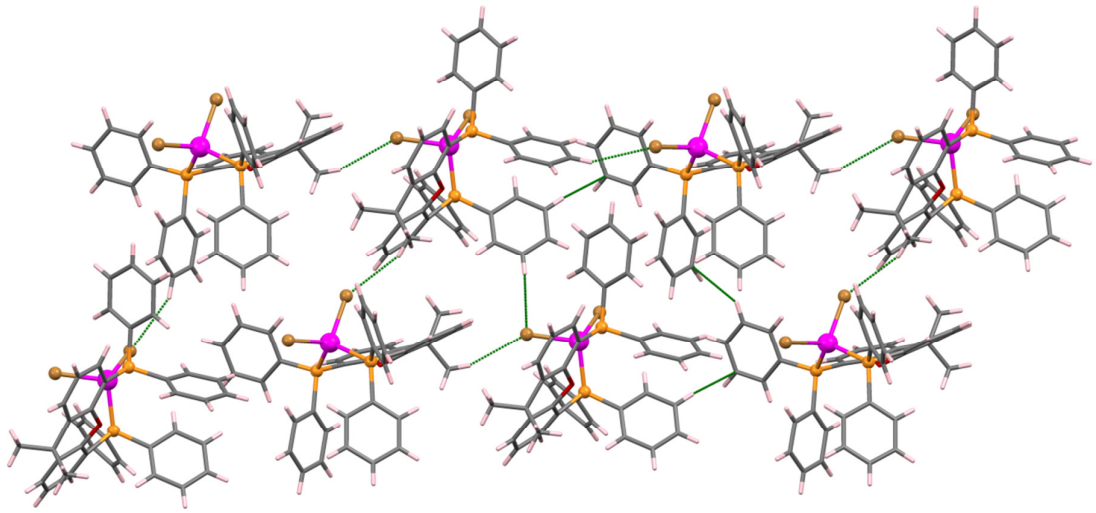

Fig. S7. A view of supramolecular 2D arrangement of complex **3** through intermolecular H-bonding and CH···π interactions.

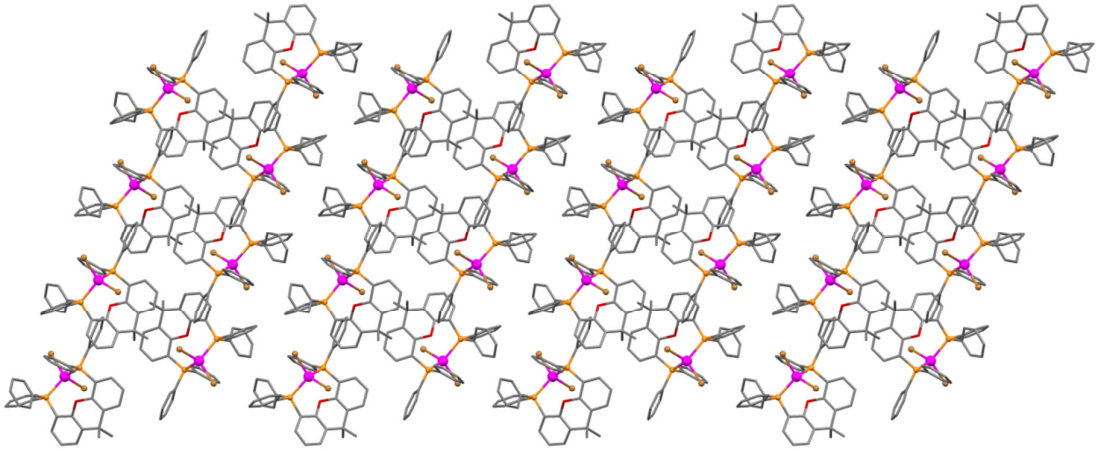

Fig. S8. Packing arrangement of complex **3** along the crystallographic *b*-axis.

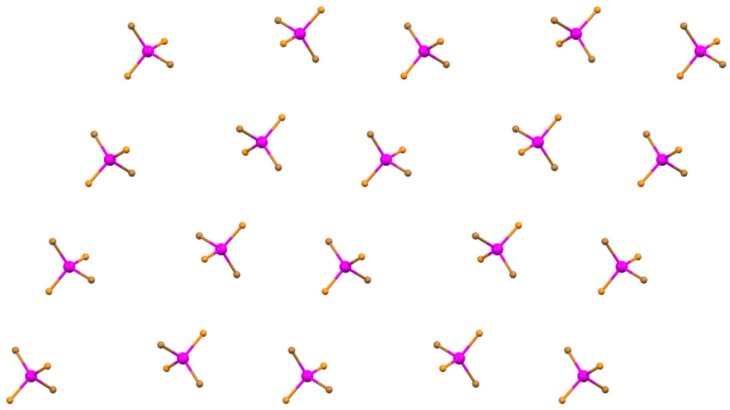

Fig. S9. Packing arrangement of complex **3** along the crystallographic *b*-axis, after removing the outer sphere ligand and keeping only the tetrahedral Co^{II} cores.

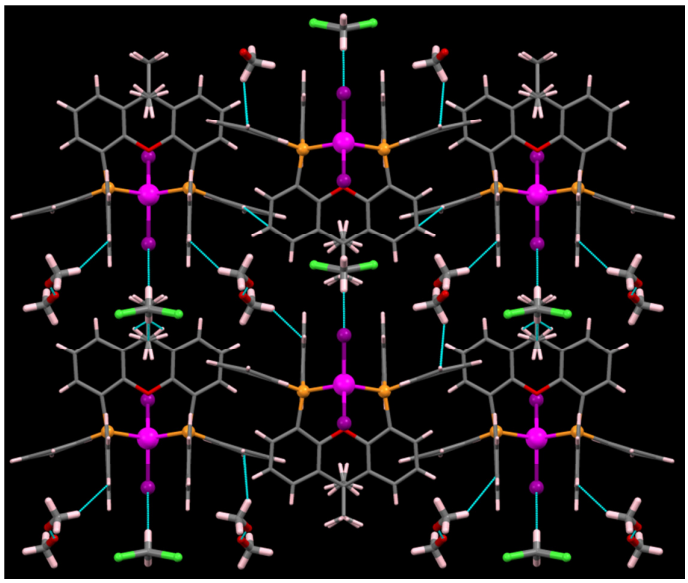

Fig. S10. A view of supramolecular 2D arrangement of complex **4** through intermolecular H-bonding and CH···π interactions.

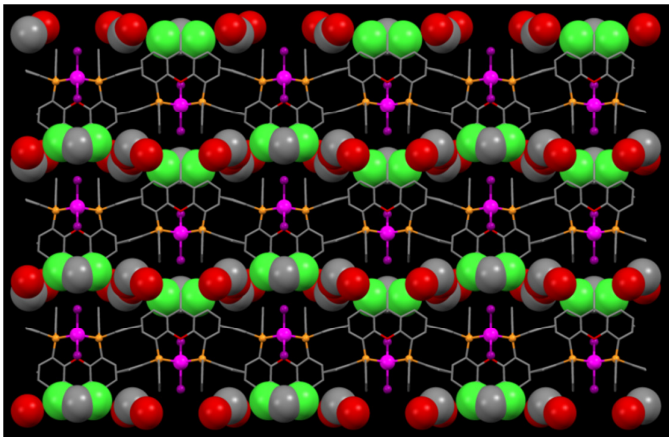

Fig. S11. A view of packing diagram of complex **4** illustrating the continuous 2D arrangement of lattice solvent molecules along the crystallographic *a*-axis.

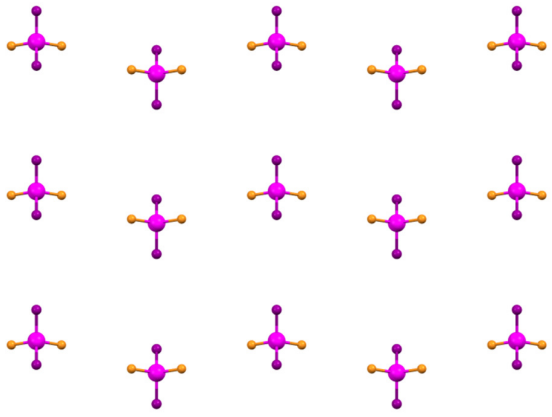

Fig. S12. Packing arrangement of complex **4** along the crystallographic *a*-axis, after removing the outer sphere ligand and keeping only the tetrahedral Co^{II} cores.

Table S5. H-bond parameters found in complex **1.**

D– H···A	D–H(Å)	H···A(Å)	D···A (Å)	<D-H-A(°)	Symmetry[#]
C21—H21···N2	0.950	2.737	2.581	156.22	0
C23—H23···N1	0.950	2.914	3.410	113.84	0
C27—H27···O1	0.950	2.779	3.348	119.32	0
C35—H35···N2	0.950	2.869	3.692	145.58	0
C33—H33···N1	0.950	2.901	3.746	148.79	0
C7—H7C···O1	0.980	2.743	3.268	114.08	0
C1—H1···S2	0.950	2.927	3.669	135.81	1
C15—H15C···S1	0.980	2.837	3.757	156.78	2
C37—H37···S1	0.950	2.984	3.865	154.83	3
C36—H36···N1	0.950	2.705	3.649	172.51	4

(0) x,y,z; (1) x+1,+y+1,z; (2) x,+y+1,+z; (3) -x+1,-y,-z+1; (4) -x,-y,-z+1.

Table S6. H-bond parameters found in complex **2.**

D– H···A	D–H(Å)	H···A(Å)	D···A (Å)	<D-H-A(°)	Symmetry[#]
C152—H152···O2	0.930	2.738	3.605	155.49	0
C120—H120···Cl6	0.930	2.868	3.710	151.25	1
C128—H128···Cl1	0.930	2.948	3.869	171.14	2
C134—H134···O3	0.930	2.727	3.596	155.98	3
C143—H14D···Cl1	0.960	2.897	3.746	148.09	4
C102—H102···C15	0.930	2.948	3.874	173.60	5
C146—H146···C15	0.930	2.858	3.773	168.31	5
C83—H83···Cl1	0.930	2.939	3.860	170.58	6

(0) x,y,z; (1) -x+1,-y,-z; (2) x,+y-1,+z; (3) x-1,+y,+z; (4) -x+1,+y-1/2,-z+1/2; (5) x,+y+1,+z; (6) x+1,+y-1,+z.

Table S7. H-bond parameters found in complex **3.**

D– H···A	D–H(Å)	H···A(Å)	D···A (Å)	<D-H-A(°)	Symmetry[#]
C116—H116···O1	0.930	2.747	3.598	152.61	0
C128—H128···O3	0.930	2.751	3.620	155.79	1
C136—H136···Br3	0.930	2.989	3.916	174.72	2
C142—H14D···Br1	0.960	2.992	3.862	151.28	3
C82—H82···Br1	0.930	2.917	3.839	171.47	4
C93—H93C···Br3	0.960	2.940	3.817	152.34	5
C102—H102···Br2	0.930	2.974	3.832	154.21	6

(0) x,y,z; (1) x-1,+y,+z; (2) x,+y-1,+z; (3) -x+1,+y+1/2,-z+1/2; (4) x+1,+y+1,+z; (5) -x+2,+y-1/2,-z+1/2; (6) -x+1,-y,-z.

Table S8. H-bond parameters found in complex **4.**

D– H···A	D–H(Å)	H···A(Å)	D···A (Å)	<D-H-A(°)	Symmetry[#]
C14—H14···O6	0.930	2.866	3.440	121.13	0
C8—H8···O1A	0.930	2.929	3.349	108.98	0
C16—H16B···O1A	0.960	2.882	3.358	111.75	0
C28—H28A···O5	0.960	1.645	2.215	113.82	0
C15—H15···O6	0.930	2.885	3.565	131.00	1
C11—H11···Cl1	0.930	2.956	3.726	141.10	2
C5—H5···Cl1	0.930	2.991	3.728	137.33	3

(0) x,y,z; (1) -x+1,-y+1,-z+2; (2) x,+y,+z-1; (3) -x,-y+1,-z+1.

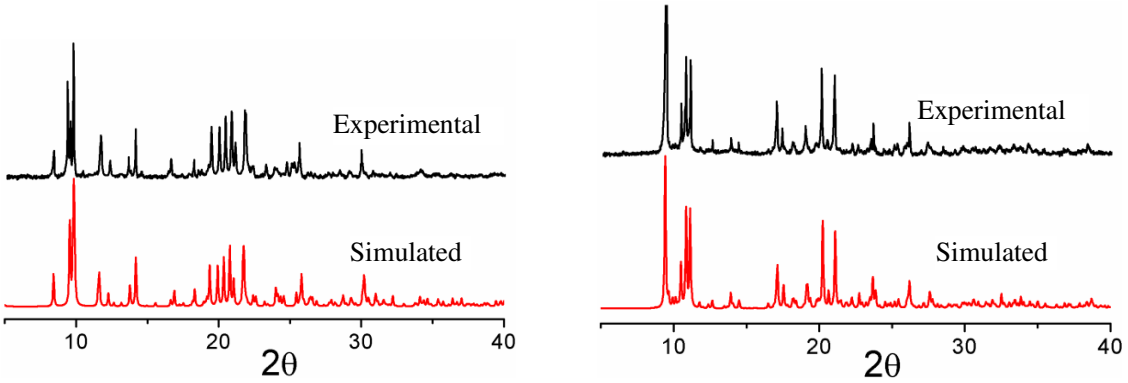

Fig. S13. PXRD patterns of complexes **1** (left) and **2** (right).

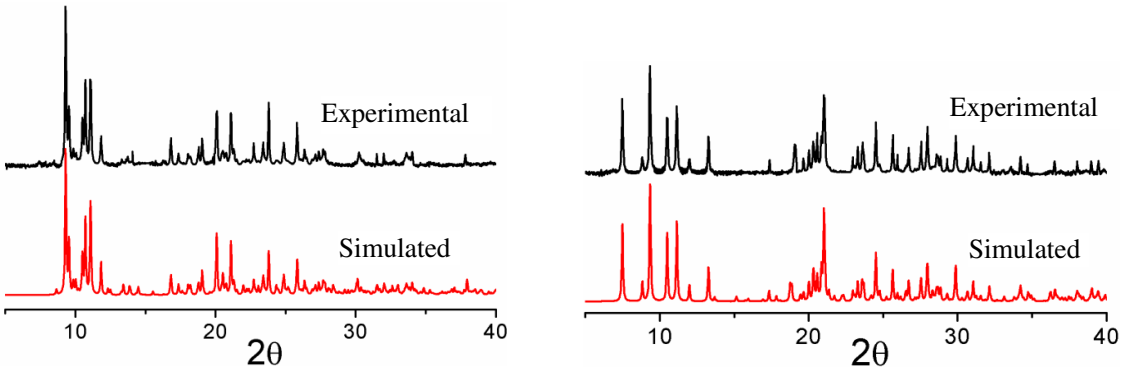

Fig. S14. PXRD patterns of complexes **3** (left) and **4** (right).

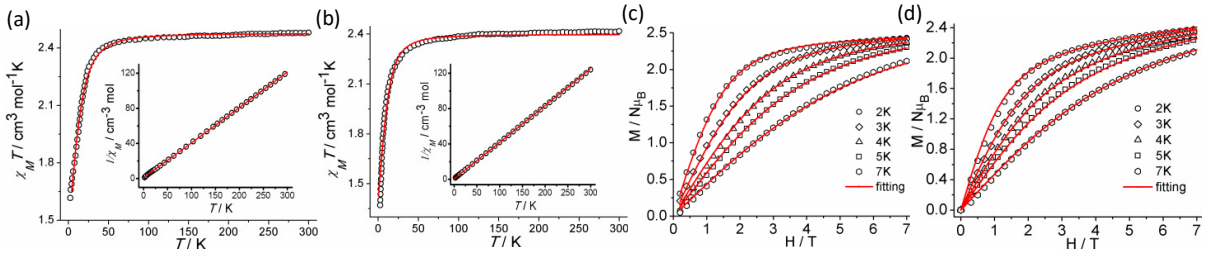

Fig. S15. $\chi_M T$ *vs.* T plots measured at 0.1 T for complex **3** (a) and **4** (b). $1/\chi_M$ *vs.* T plots shown in the inset; $M/N\mu_B$ *vs.* H plots for complex **3** (c) and **4** (d) at the indicated temperatures. The red lines are the best fit.

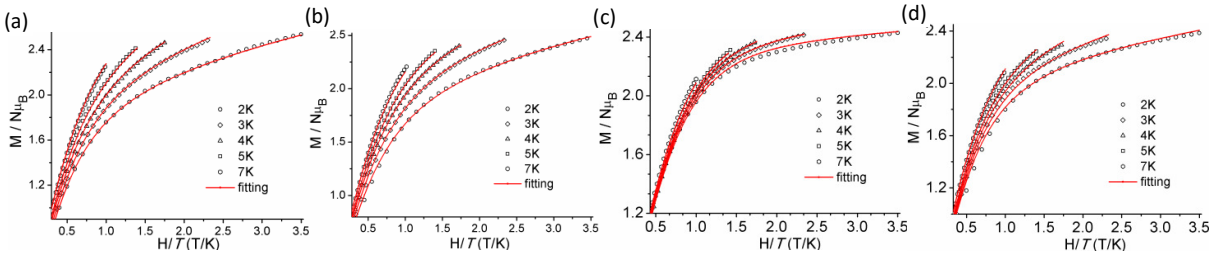

Fig. S16. $M/N\mu_B$ *vs. H/T* plots at the indicated temperatures for complexes **1-4** (a-d). The red lines are the best fit.

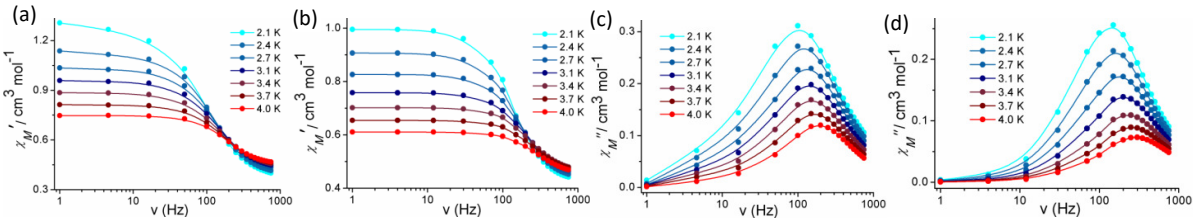

Fig. S17. Frequency dependency of the in-phase (χ_M') (a and b) and out-of-phase (χ_M'') (c and d) AC magnetic susceptibility plots for complex **3** and **4** under 1000 Oe dc field.

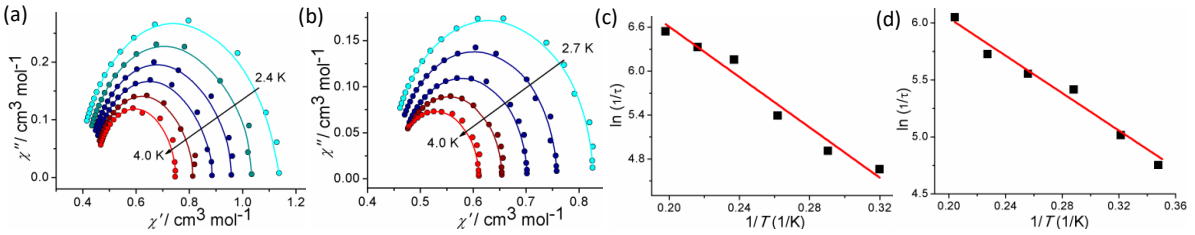

Fig. S18. Cole-Cole plots for complex **3** (a) and **4** (b). Solid lines represent the best fit; ln ($1/\tau$) *vs.* $1/T$ plots for complex **3** (c) and **4** (d). The red lines are the best fit of the Arrhenius relationship.

Experimental information for dilution studies:

Synthesis of [Zn(L)(Cl)$_2$] (5)

Ligand (57 mg, 0.1 mmol) was dissolved in CH_2Cl_2 (5 ml) and the solution was stirred at room temperature. Then, $ZnCl_2$ (14 mg, 0.1 mmol) dissolved in MeOH (5 ml) was added dropwise to the above ligand solution. The resulting solution forms an intense blue mixture that was stirred further for 2 hrs. The solution was then filtered off and the filtrate was left at open atmosphere for slow evaporation which yields large X-ray quality yellow crystals of [Zn(L)(Cl)$_2$] (**5**) after 2 days. The crystals were separated, washed with cold water and Et_2O and air-dried yield (70 %). Anal. Calcd for $C_{39}H_{32}ZnCl_2P_2O$: C, 65.50; H, 4.51 %. Found: C, 65.57; H, 4.42 %.

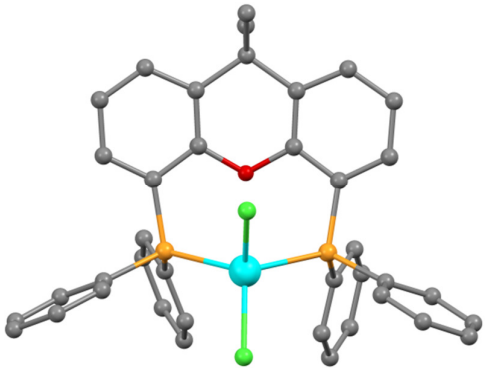

Fig. S19. View of the molecular structure of complex **5**; hydrogen atoms are omitted for clarity.

Table S9. X-ray Crystallographic Data and Refinement Parameters for complex **5**.

	5
Formula	$C_{39}H_{32}ZnCl_2P_2O$
M_w (g mol^{-1})	714.88
Crystal size (mm)	0.45×0.18×0.16
Crystal system	Monoclinic
Space group	$P2_1/c$
T (K)	296(2)
a (Å)	16.8819(5)
b (Å)	10.4934(3)
c (Å)	40.2603(12)
α (°)	90
β (°)	111.192(2)
γ (°)	90
V (Å^3)	6649.7(3)
Z	8
ρ_{calcd} (g cm^{-3})	1.428
μ(MoKα) (mm^{-1})	1.027
F(000)	2944.0
T_{max}, T_{min}	0.838, 0.811
h, k, l range	$-22 \le h \le 22$, $-14 \le k \le 14$, $-54 \le l \le 54$
Collected reflections	17263
Independent reflections	11399
Goodness-of-fit (GOF) on F^2	0.872
R1, wR2 ($I > 2\sigma I$)	0.0456, 0.1054
R1, wR2 (all data)	0.0800, 0.1234
CCDC Number	1527508

$R1 = \Sigma||Fo| - |Fc||/\Sigma|Fo|$ and $wR2 = |\Sigma w(|Fo|^2 - |Fc|^2)|/\Sigma|w(Fo)^2|^{1/2}$

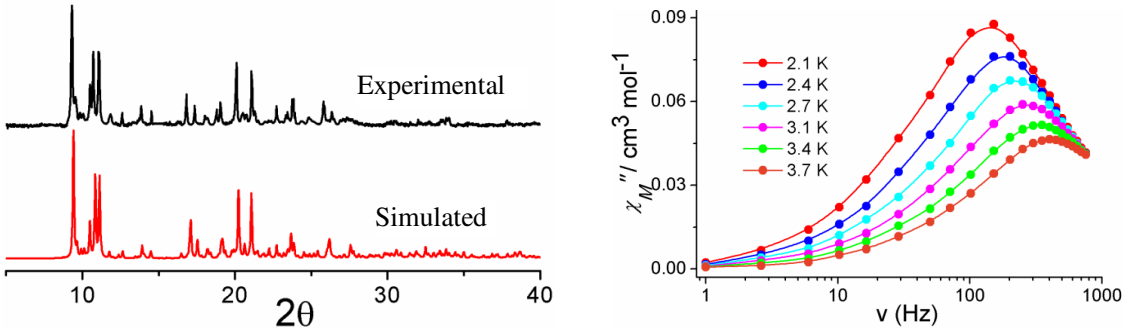

Fig. S20. PXRD patterns of diluted sample (left); Frequency dependency of the out-of-phase (χ_M'') AC magnetic susceptibility plot for diluted sample at 1000 Oe dc field (right).

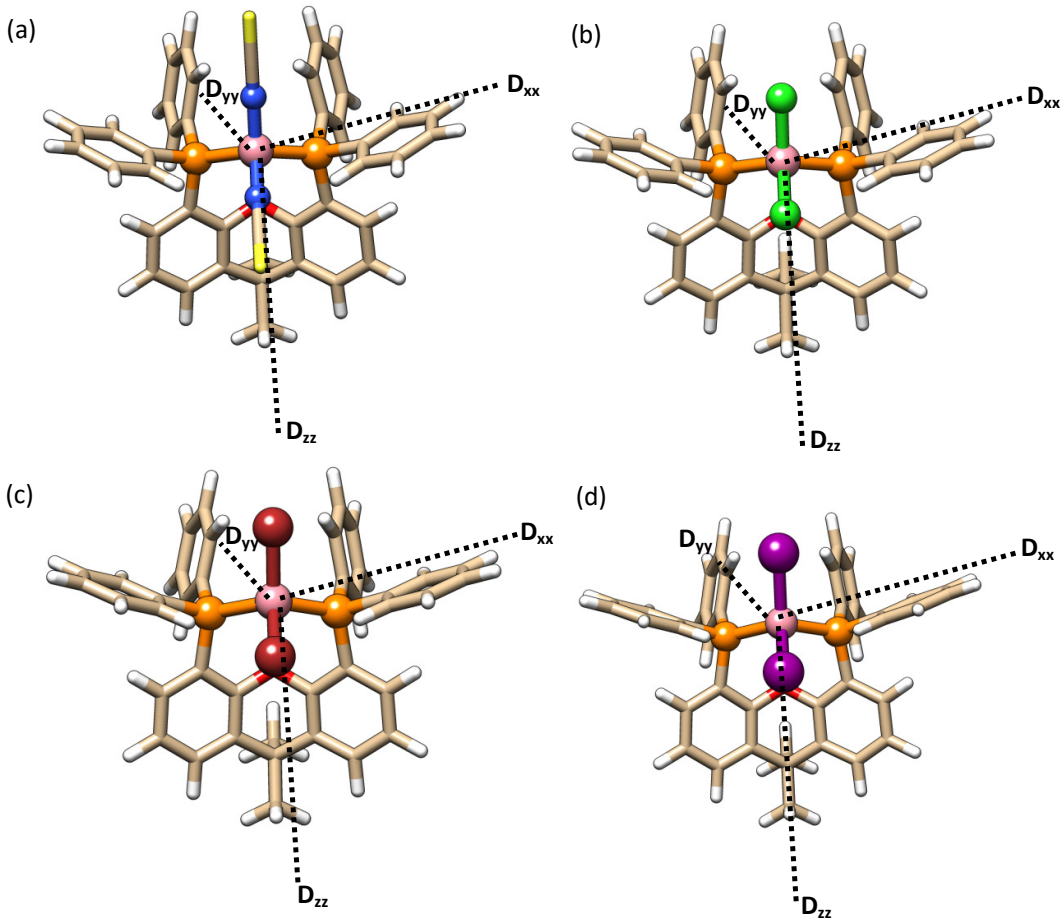

Fig. S21. Optimized structure of complexes **1**-**4** (a-d) at the DFT level along with *ab initio* computed *D*-tensor orientation.

Table S10. Optimized structural parameters of complexes **1**-**4**.[a]

	1	**2**	**3**	**4**
Co-P, Å	2.345,2.345 (2.372)	2.339 (2.378)	2.336,2.337 (2.366)	2.337,2.338 (2.364)
Co-X, Å	1.873, 1.869 (1.924)	2.215, 2.223 (2.221)	2.352, 2.363 (2.356)	2.542, 2.554 (2.554)
α, °	114.33 (112.82)	115.51 (114.22)	115.14 (114.67)	114.97 (112.92)
β, °	121.48 (114.70)	118.50 (116.34)	117.15 (116.57)	114.95 (118.53)

[a] Values in brackets are from experiments

Table S11. AILFT and the ligand field splitting parameters for the four complexes (in cm^{-1}).

	1	**2**	**3**	**4**
Δ	-5864	-4897	-4459	-4057
10*Dq*	5324 (4967)	4424 (4333)	4149 (4333)	3849 (4033)
μ	-541	-473	-310	-207
B	940	948	945	932
β[a]	0.869	0.876	0.873	0.861
C	3880	3939	3944	3916
Z	505.2	504.0	495.5	473.4

[a]$\beta=B/B_0$, B_0 = Racah parameter of free Co^{2+} ion = 1082 cm^{-1} (1120 cm^{-1})

Table S12. Comparison of the experimental absorption maxima and calculated electronic transition energies [a] (in cm^{-1}).

level	**1**	**2**	**3**	**4**
$^4A_2 \rightarrow {}^4T_2(F)$	4400 (5092.1)	4000 (4248.4)	4000 (4094.7)	3800 (3834.1)
$^4A_2 \rightarrow {}^4T_2(F)$	4800 (5455.5)	4300 (4450.6)	4300 (4220.5)	4000 (4298.3)
$^4A_2 \rightarrow {}^4T_2(F)$	5700 (7567.2)	4700 (6140.8)	4700 (5862.2)	4300 (5563.5)
$^4A_2 \rightarrow {}^4T_1(F)$	7600 (8221.6)	6200 (7385.0)	5900 (7258.7)	5700 (7242.0)
$^4A_2 \rightarrow {}^4T_1(F)$	8400 (10011.2)	7400 (8744.2)	6900 (8428.8)	6800 (8254.6)
$^4A_2 \rightarrow {}^4T_1(F)$	9350 (13232.7)	9050 (11941.4)	8800 (11526.5)	8650 (11172.5)
$^4A_2 \rightarrow {}^4T_1(P)$	16200 (17971.2)	15700 (17934.2)	15400 (18306.6)	14500 (18829.9)
$^4A_2 \rightarrow {}^4T_1(P)$	16800 (22159.3)	16400 (21057.3)	16100 (20611.1)	15200 (20221.3)
$^4A_2 \rightarrow {}^4T_1(P)$	17800 (23849.2)	17100 (21959.0)	16500 (21071.1)	16000 (20281.8)

[a] calculated values in brackets.